

Centrality dependence of v_2 in Au + Au at $\sqrt{s_{NN}} = 200$ GeV

Unidentified charged hadron v_2 with respect to the first harmonic ZDC-SMD event plane

Hiroshi Masui^a
for the PHENIX Collaboration

Nuclear Science Division, Lawrence Berkeley National Laboratory, 1 Cyclotron Road, Berkeley, CA 94720, USA

Received: 30 September 2008 / Revised: 7 February 2009 / Published online: 8 April 2009
© Springer-Verlag / Società Italiana di Fisica 2009

Abstract One of the most striking results is the large elliptic flow (v_2) at RHIC. Detailed mass and transverse momentum dependence of elliptic flow are well described by ideal hydrodynamic calculations for $p_T < 1$ GeV/c, and by parton coalescence/recombination picture for $p_T = 2\text{--}6$ GeV/c. The systematic error on v_2 is dominated by so-called “non-flow effects”, which are correlations other than flow, such as resonance decays and jets. It is crucial to understand and reduce the systematic error from non-flow effects in order to understand the underlying collision dynamics. In this paper, we present the centrality dependence of v_2 with respect to the first harmonic event plane at ZDC-SMD ($v_2\{\text{ZDC-SMD}\}$) in Au + Au collisions at $\sqrt{s_{NN}} = 200$ GeV. A large rapidity gap ($|\Delta\eta| > 6$) between midrapidity and the ZDC-SMD could enable us to minimize possible non-flow contributions. We compare the results of $v_2\{\text{ZDC-SMD}\}$ with $v_2\{\text{BBC}\}$, which is measured by event plane determined at $|\eta| = 3.1\text{--}3.9$. Possible non-flow contributions in those results will be discussed.

PACS 25.75.-q · 25.75.Ld

1 Introduction

Elliptic flow is expected to be one of the key observables to study an early stage of heavy ion collisions [1]. It is defined by the second harmonic Fourier coefficient

$$v_2 = \langle \cos(2[\phi - \Psi_{RP}]) \rangle, \quad (1)$$

where ϕ is the azimuthal angle of emitted particles, Ψ_{RP} is the azimuthal angle of the reaction plane and brackets denote the average over all particles and events.

^a e-mail: HMasui@lbl.gov

The PHENIX experiment at Relativistic Heavy Ion Collider (RHIC) has measured the v_2 for identified charged hadrons [2, 3], ϕ mesons and deuterons [4], π^0 's and photons [5] as well as electrons from heavy flavor decays [6] at midrapidity. The mass ordering of v_2 for identified hadrons was qualitatively explained by ideal hydrodynamics in the transverse momentum $p_T < 2$ GeV/c [2]. For intermediate $p_T = 2\text{--}6$ GeV/c, a universal parton v_2 was obtained by dividing v_2 and p_T by the number of constituent quarks for each hadron [2, 3]. The v_2 for ϕ meson was also found to follow the quark number scaling, which support that the parton v_2 has already developed prior to the hadronization [4]. Because the hadronic cross section between ϕ meson and other non-strange hadrons is small, the v_2 of ϕ meson is less sensitive to the late hadronic stage. The finite v_2 for electrons from heavy flavor decays implies a non-zero charm v_2 [6]. Comparison of v_2 with transport model calculation suggest that the viscosity to entropy density ratio is close to the quantum lower bound $1/4\pi$ [7].

These measurements were done by using an event plane determined from the Beam-Beam Counter (BBC) located at pseudorapidity $|\eta| = 3.1\text{--}3.9$. The large pseudorapidity separation $|\Delta\eta| \sim 3$ from midrapidity would reduce non-flow effects. The non-flow effects are correlations other than flow such as jets, resonance decays and so on. Fluctuations of v_2 were also considered as the non-flow contributions [8], which would become more important in smaller systems, such as Cu + Cu collisions.

In this paper, we present the v_2 with respect to the event plane from directed flow determined at the Shower Maximum Detector (ZDC-SMD), which is located at $|\eta| > 6$. Since the larger rapidity separation could reduce the possible non-flow effects on our measured v_2 , the v_2 of ZDC-SMD could quantify how the BBC event plane is sensitive to the non-flow effects. We will compare the v_2 results from

the event planes determined at the BBC and ZDC-SMD and discuss the possible non-flow contributions on the v_2 .

2 Data analysis

In this study, we analyzed $\sim 650M$ events collected by the PHENIX experiment in Au + Au at $\sqrt{s_{NN}} = 200$ GeV. Minimum bias events were selected within a collisions z-vertex ± 30 cm. Event centrality was determined by the correlation between the energy deposited at the Zero Degree Calorimeter (ZDC) and the number of charged particles at the BBC. Tracking was done by the Drift Chamber (DC) and Pad Chambers (PCs) at the central arm $|\eta| < 0.35$. Transverse momentum was determined by the incident angle at the DC. The polar angle of the tracks was obtained by the hit at the inner PC (PC1) and the collision vertex from the BBC. Track associations were made by comparing hit positions with the projection of the DC tracks to the outer Pad Chamber (PC3). Tracks were required to have a hit on the PC3 within $\pm 3\sigma$ of the expected hit location in both azimuthal and beam directions. Momentum dependent energy cut $E/p > 0.2$ at the Electromagnetic Calorimeter (EMCal) were also required, where E is the energy deposited in EMCal and p is the momentum determined at the DC in order to reduce photon conversions for $p_T > 4$ GeV/c [9]. Since background electrons are mostly low p_T , large energy deposited in the EMCal is effective to suppress the electron backgrounds.

The v_2 was measured by an event plane method [10] and was obtained by dividing the measured v_2 by the event plane resolution

$$v_2 = \frac{v_2^{obs}}{\text{Res}\{\Psi_n\}} = \frac{\langle \cos(2[\phi - \Psi_n]) \rangle}{\langle \cos(2[\Psi_n - \Psi_{RP}]) \rangle}, \quad (2)$$

where ϕ is the azimuth of charged hadrons at the central arm ($|\eta| < 0.35$), Ψ_n is the event plane from the n -th harmonic flow ($n = 1$ for the ZDC-SMD, $n = 2$ for the BBC) and v_2^{obs} is the measured v_2 with respect to the event plane Ψ_n . Event planes were determined from the v_2 at the BBC and the central arm as well as the directed flow $v_1 = \langle \cos(\phi - \Psi_{RP}) \rangle$ at the Shower Maximum Detector (SMD). The central arm event plane is only used to evaluate the event plane resolutions. The SMDs are located at the same acceptance of the ZDCs, $|\eta| > 6$, and measure transverse positions of spectator neutrons. The measured v_2 's are denoted as $v_2\{\text{ZDC-SMD}\}$ and $v_2\{\text{BBC}\}$ for the ZDC-SMD and BBC event planes, respectively.

The event plane determined at the ZDC-SMD can minimize non-flow correlations as well as v_2 fluctuations because of the following reasons. First, the pseudorapidity gap from midrapidity is 6, which is higher than what we have

previously studied by using the BBC. Second, the ZDC-SMD event plane is determined from directed flow. This mixed harmonic method involves three particle correlations and thus direct two particle correlations, which is dominated by contributions from non-flow effects, do not affect the measured v_2 by reflection symmetry between azimuth of particles and the event plane. Third, ZDC-SMD measures spectator neutrons rather than participants. Therefore, v_2 fluctuations are suppressed up to the fluctuation of spectator neutrons.

Figure 1 shows the event plane resolutions as a function of centrality. At least two independent event planes are required in order to evaluate the resolution since the azimuth of true reaction plane is unknown. The resolution from two independent event planes is calculated by

$$\text{Res}\{\Psi_n\} = C \sqrt{\langle \cos(2[\Psi_n^- - \Psi_n^+]) \rangle}, \quad (3)$$

where Ψ_n^+ and Ψ_n^- denote the event planes determined at the forward and backward pseudorapidities, respectively. A constant parameter C is very close to $\sqrt{2}$ for both BBC and ZDC-SMD due to low resolution [10]. The ZDC-SMD resolution is about a factor of 4 smaller than that of BBC because the ZDC-SMD event plane is determined from directed flow. It is approximately proportional to $v_1^2 M^{\text{SMD}}$, where M^{SMD} is the multiplicity used to determine the ZDC-SMD event plane, whereas the BBC resolution is roughly proportional to $v_2 \sqrt{M^{\text{BBC}}}$.

The resolutions were also evaluated by adding a reference event plane

$$\text{Res}\{\Psi_n\} = \sqrt{\frac{\langle \cos(2[\Psi_l^A - \Psi_n]) \rangle \langle \cos(2[\Psi_n - \Psi_m^B]) \rangle}{\langle \cos(2[\Psi_m^B - \Psi_l^A]) \rangle}}, \quad (4)$$

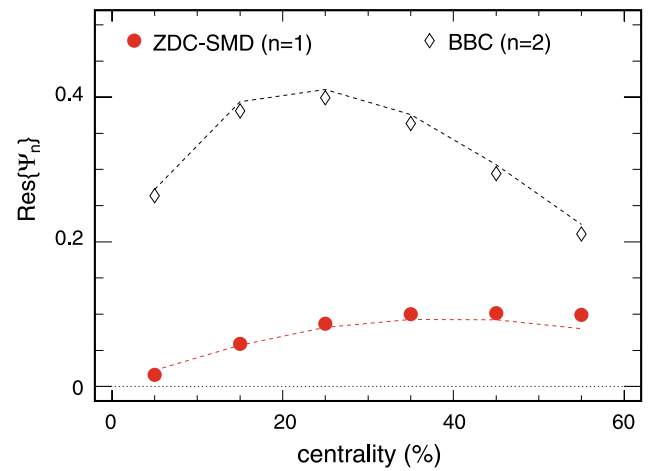


Fig. 1 Event plane resolutions as a function of centrality for the ZDC-SMD event plane (solid circles) and the BBC (open diamonds) by (3). Dashed lines represent the resolutions calculated by (4)

where l , m and n denote the harmonics for event plane Ψ^A , Ψ^B and Ψ , respectively. Dashed lines in Fig. 1 show the resolutions calculated by (4). For example, the BBC resolution was calculated by inserting $\Psi_n = \Psi_2^{\text{BBC}}$, $\Psi_l^A = \Psi_1^{\text{ZDC-SMD}}$, and $\Psi_m^B = \Psi_2^{\text{CNT}}$ where CNT denote the central arm. One can find that the dashed lines are systematically lower for the ZDC-SMD, and higher for the BBC. The comparison of v_2 from two different resolutions will be presented in the next section.

3 Results

We will present the preliminary results of $v_2\{\text{BBC}\}$ as well as $\{\text{ZDC-SMD}\}$ in Au + Au collisions at $\sqrt{s_{NN}} = 200$ GeV measured at the PHENIX experiment. Sect. 3.1 will give comparison of the v_2 between BBC and ZDC-SMD event planes. Results between PHENIX and STAR experiments will be compared in Sect. 3.2. In Sect. 3.3, centrality dependence of the $v_2\{\text{ZDC-SMD}\}$ will be compared with the $v_2\{\text{BBC}\}$.

3.1 Comparison of $v_2\{\text{BBC}\}$ with $v_2\{\text{ZDC-SMD}\}$

Figure 2 shows the $v_2\{\text{ZDC-SMD}\}$ as a function of p_T in 20–60% centrality. For comparison, the $v_2\{\text{BBC}\}$ is also plotted by open diamonds. The v_2 increases linearly up to $p_T \sim 3$ GeV/c, reaches a maximum at ~ 0.2 and then starts decreasing for higher p_T . The $v_2\{\text{ZDC-SMD}\}$ (S-N), which is obtained from the resolution in (3), is about 7% systematically lower than the $v_2\{\text{BBC}\}$, while the results are consistent within systematic uncertainties. We also plot the $v_2\{\text{ZDC-SMD}\}$ (ZDC-BBCS-BBCN) as shown by solid circles, which is obtained from the resolution in (4) by inserting $\Psi_n = \Psi_1^{\text{ZDC-SMD}}$, $\Psi_n^A = \Psi_2^{\text{BBCS}}$ and $\Psi_n^B = \Psi_2^{\text{BBCN}}$. The BBCS and BBCN denote the backward and forward BBC, respectively. The $v_2\{\text{ZDC-SMD}\}$ from two different resolutions are in good agreement within systematic uncertainties. Bottom panel shows the ratio of $v_2\{\text{ZDC-SMD}\}$ to $v_2\{\text{BBC}\}$ as a function of p_T . One can see that the ratio is constant within systematic errors in the measured p_T range.

3.2 PHENIX vs. STAR

Figure 3 show the comparison of the PHENIX $v_2\{\text{ZDC-SMD}\}$ with STAR results [11] in 20–60% centrality bin. Only statistical errors are shown for the STAR v_2 . Both PHENIX and STAR results are obtained by the resolution in (3) and thus the results of $v_2\{\text{ZDC-SMD}\}$ are extracted by the exactly same method. Data symbols (open diamonds and open crosses) are the same as shown in Fig. 2. For a quantitative comparison, the ratio of v_2 to the $v_2\{\text{BBC}\}$ is

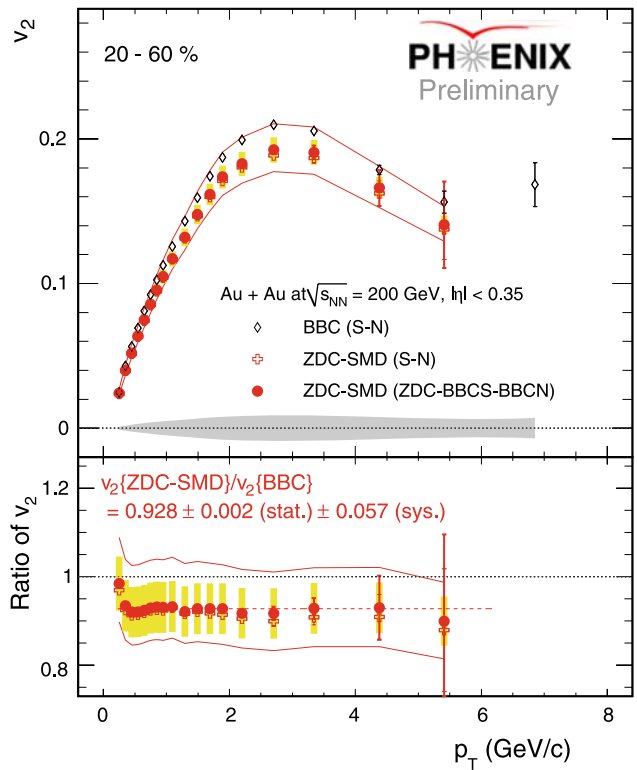


Fig. 2 (Color online) (Top) Comparison of v_2 as a function of p_T in 20–60% centrality for the BBC (open diamonds), the ZDC-SMD from two different event plane resolutions (open crosses and solid circles, see texts). Gray bands, solid red lines and yellow boxes represent systematic uncertainties on the $v_2\{\text{BBC}\}$ and $v_2\{\text{ZDC-SMD}\}$. (Bottom) The ratio of $v_2\{\text{ZDC-SMD}\}$ to $v_2\{\text{BBC}\}$ as a function of p_T . Systematic errors on the ratio denote the quadratic sum of the $v_2\{\text{BBC}\}$ and $v_2\{\text{ZDC-SMD}\}$. Dashed line denotes the fit result by constant

plotted in the bottom panel in Fig. 3. The denominator of the ratio is the results of the fit of the $v_2\{\text{BBC}\}$ by fourth-order polynomial function. One can see that the results agree very well within systematic errors.

3.3 Centrality dependence of v_2

Figure 4 show the $v_2(p_T)$ in centrality 20–60%. In Fig. 4(a), the $v_2\{\text{ZDC-SMD}\}$ is consistent with the $v_2\{\text{BBC}\}$ within systematic errors in centrality 20–40%. In peripheral 40–60%, we find that the $v_2\{\text{ZDC-SMD}\}$ is 5–10% lower than the $v_2\{\text{BBC}\}$. The lower $v_2\{\text{ZDC-SMD}\}$ could suggest possible non-flow contributions on the $v_2\{\text{BBC}\}$. We also find that the $v_2\{\text{ZDC-SMD}\}$ become closer with the $v_2\{\text{BBC}\}$ by estimating the resolutions with the ZDC-BBC-CNT combination as shown in Fig. 4(b). As we have shown in Fig. 1, the (4) decrease the resolution for the ZDC-SMD and increase the resolution for the BBC by using the ZDC-BBC-CNT combination. This raise the $v_2\{\text{ZDC-SMD}\}$ and lower the $v_2\{\text{BBC}\}$, and thus they become closer together compared to those from the S-N combination in Fig. 4(a). The cause of the difference of the v_2 between Figs. 4(a) and

(b) could be due to the possible non-flow effects and the v_2 fluctuations on the measured v_2 as well as on the event plane resolutions. A simulation study has shown that the bias

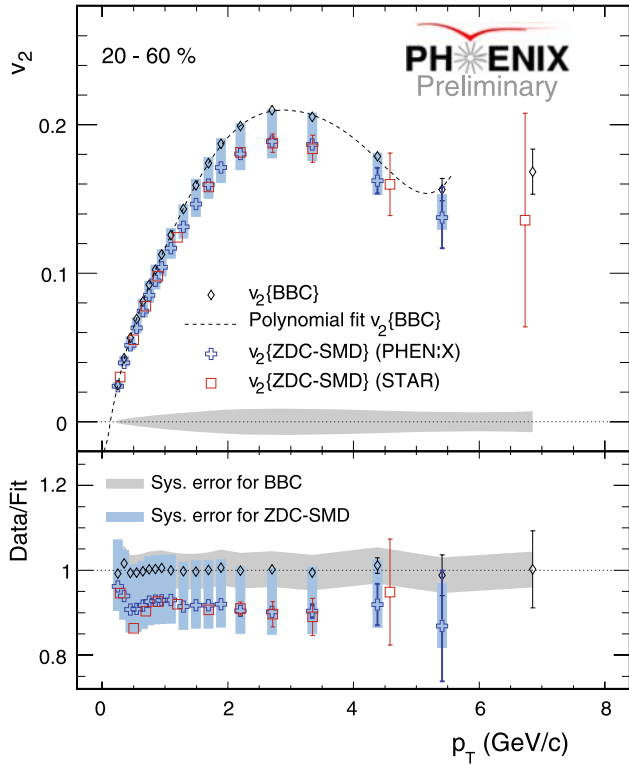


Fig. 3 (Color online) Comparison of the $v_2\{\text{ZDC-SMD}\}$ between PHENIX and STAR experiments in 20–60% centrality. The STAR $v_2\{\text{ZDC-SMD}\}$ is taken from [11]. Gray bands and light blue boxes denote the systematic uncertainties on the $v_2\{\text{BBC}\}$ and $v_2\{\text{ZDC-SMD}\}$, respectively. Bottom panel shows the ratio of v_2 to the fourth-order polynomial fit of the $v_2\{\text{BBC}\}$ as a function of p_T

from the dijet are negligible in the BBC acceptance [12]. Since The dijet is expected to be a major contribution on the non-flow effects at high p_T , this study suggest the $v_2\{\text{ZDC-SMD}\}$ is also insensitive to the dijet due to the larger rapidity separation compared to the BBC. Therefore the difference of the v_2 may be dominated by the v_2 fluctuations. A further study will be needed in order to evaluate quantitatively the effect of v_2 fluctuations and non-flow contributions.

4 Conclusion

In summary, we have measured unidentified charged hadron elliptic flow with respect to the ZDC-SMD event plane from directed flow in Au + Au at $\sqrt{s_{NN}} = 200$ GeV. The $v_2\{\text{ZDC-SMD}\}$ was compared with the v_2 measured with respect to the event plane determined at the BBC. We found that the $v_2\{\text{ZDC-SMD}\}$ was consistent with the $v_2\{\text{BBC}\}$ within systematic uncertainties in centrality 20–40%. The difference of v_2 between BBC and ZDC-SMD event planes is $\sim 5\text{--}10\%$ at 40–60% centrality bins could attribute to the possible non-flow effects. We found that resulting $v_2\{\text{ZDC-SMD}\}$ was still consistent with the $v_2\{\text{BBC}\}$ even if the CNT event plane was included in the event plane resolution. These result gives an upper limit of non-flow contributions is about 5–10% in centrality 40–60% by assuming if the difference of the v_2 is totally due to the non-flow effects. The v_2 fluctuations could be the cause of the difference between the BBC and ZDC-SMD if the non-flow effects are negligible in the BBC.

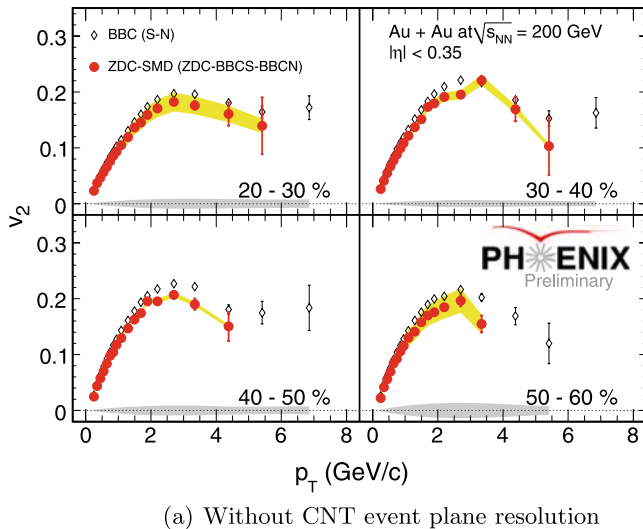
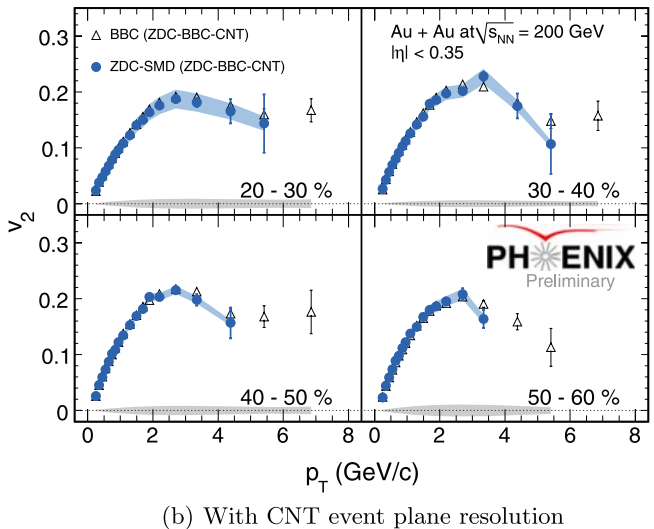


Fig. 4 Comparison of $v_2\{\text{ZDC-SMD}\}$ to $v_2\{\text{BBC}\}$ as a function of p_T in centrality 20–60%, where each centrality bin contains 10% of the total cross section. (a), (b) Results without and with the central arm (CNT) event plane resolution, respectively



References

1. J.Y. Ollitrault, Phys. Rev. D **46**, 229 (1992)
2. S.S. Adler et al. (The PHENIX Collaboration). Phys. Rev. Lett. **91**, 182301 (2003). [nucl-ex/0305013](#)
3. A. Adare et al. (The PHENIX Collaboration). Phys. Rev. Lett. **98**, 162301 (2007). [nucl-ex/0608033](#)
4. S. Afanasiev et al. (The PHENIX Collaboration). Phys. Rev. Lett. **99**, 052301 (2007). [nucl-ex/0703024](#)
5. S.S. Adler et al. (The PHENIX Collaboration). Phys. Rev. Lett. **96**, 032302 (2006). [nucl-ex/0508019](#)
6. S.S. Adler et al. (The PHENIX Collaboration). Phys. Rev. C **72**, 024901 (2005). [nucl-ex/0502009](#)
7. A. Adare et al. (The PHENIX Collaboration). Phys. Rev. Lett. **98**, 172301 (2007). [nucl-ex/0611018](#)
8. C. Adler et al. (The STAR Collaboration). Phys. Rev. C **66**, 034904 (2002). [nucl-ex/0206001](#)
9. S.S. Adler et al. (The PHENIX Collaboration). Phys. Rev. C **73**, 054903 (2006). [nucl-ex/0510021](#)
10. A.M. Poskanzer, S.A. Voloshin, Phys. Rev. C **58**, 1671 (1998). [nucl-ex/9805001](#)
11. G. Wang, PhD thesis. Kent State University (2006)
12. J. Jia (The PHENIX Collaboration). Nucl. Phys. A **783**, 501 (2007). [nucl-ex/0609009](#)